AD_____

Award Number: DAMD17-01-1-0513

TITLE: Signal Detection Theory-based Information Processing for the Detection of Breast Cancer at Microwave Frequencies

PRINCIPAL INVESTIGATOR: Loren W. Nolte, Ph.D.
Liewei Sha

CONTRACTING ORGANIZATION: Duke University
Durham, North Carolina 27708-0077

REPORT DATE: August 2002

TYPE OF REPORT: Annual

PREPARED FOR: U.S. Army Medical Research and Materiel Command
Fort Detrick, Maryland 21702-5012

REPORT DOCUMENTATION PAGE

Form Approved
OMB No. 074-0188

1. AGENCY USE ONLY (Leave blank)	2. REPORT DATE	3. REPORT TYPE AND DATES COVERED
	August 2002	Annual (1 Aug 01 - 31 Jul 02)

4. TITLE AND SUBTITLE
Signal Detection Theory-based Information Processing for the Detection of Breast Cancer at Microwave Frequencies

5. FUNDING NUMBERS
DAMD17-01-1-0513

6. AUTHOR(S)
Loren W. Nolte, Ph.D.
Liewei Sha

7. PERFORMING ORGANIZATION NAME(S) AND ADDRESS(ES)
Duke University
Durham, North Carolina 27708-0077

E-Mail: lwn@ee.duke.edu

8. PERFORMING ORGANIZATION REPORT NUMBER

9. SPONSORING / MONITORING AGENCY NAME(S) AND ADDRESS(ES)
U.S. Army Medical Research and Materiel Command
Fort Detrick, Maryland 21702-5012

10. SPONSORING / MONITORING AGENCY REPORT NUMBER

11. SUPPLEMENTARY NOTES
report contains color

12a. DISTRIBUTION / AVAILABILITY STATEMENT
Approved for Public Release; Distribution Unlimited

12b. DISTRIBUTION CODE

13. Abstract ***(Maximum 200 Words)*** *(abstract should contain no proprietary or confidential information)*
The hypothesis is that one can use signal detection theory to improve the performance in detecting tumors in the breast by using this theory to develop task-oriented information processing techniques that address directly the decision-theoretic tasks of detection, localization, and classification of the tumor as malignant or benign. This technique will be developed in the framework of the microwave imaging modality, which has the advantages that the low levels of power result in no known radiation danger, there are no contrast agents, and the examinations are comfortable, i.e. no breast compressions, for the patient. Although there is considerable scattering of a microwave signal in tissue, the presence, location, and nature of tumors is "coded" in the combination of amplitude and phases in the signal energy received at multiple sensors. In this research project a tissue-model-based signal detection theory approach for the detection of mammary tumors in the presence of normal tissue will be developed and tested. Using the ROC and other performance measures, and simulation, preliminary bounds on the performance attainable for various uncertainties in malignant tissue properties (permittivity), sizes, location, and signal-to-noise ratios will be obtained.

14. SUBJECT TERMS	15. NUMBER OF PAGES
breast cancer, signal detection, microwave imaging	19
	16. PRICE CODE

17. SECURITY CLASSIFICATION OF REPORT	18. SECURITY CLASSIFICATION OF THIS PAGE	19. SECURITY CLASSIFICATION OF ABSTRACT	20. LIMITATION OF ABSTRACT
Unclassified	Unclassified	Unclassified	Unlimited

Table of Contents

Introduction

Microwave imaging is a promising new modality for breast cancer diagnosis, partly because it is non-invasive and the permittivity contrast between normal and malignant breast tissues is high [Sha, graduate student on this project, Ref.1]. In addition, the attenuation of EM propagation in normal breast tissues is low so that it can penetrate into the depth of the tissue [Sha, Ref. 1]. The hypothesis is that one can use signal detection theory to improve the performance in detecting tumors in the breast by using this theory to develop task-oriented information processing techniques that address directly the decision-theoretic tasks of detection, localization, and classification of the tumor as malignant or benign. This technique is being developed in the framework of the microwave imaging modality, which has the advantages that the low levels of power result in no known radiation danger, there are no contrast agents, and the examinations are comfortable, i.e. no breast compressions, for the patient. Although there is considerable scattering of a microwave signal in tissue, the presence, location, and nature of tumors is "coded" in the combination of amplitude and phases in the signal energy received at multiple sensors. Signal detection theory provides a framework for incorporating knowledge of tissue characteristics, and its uncertainty, directly into the design of task oriented information processors. In this research project a tissue-model-based signal detection theory approach for the detection of mammary tumors in the presence of normal tissue is being developed and tested. Using the ROC and other performance measures, and simulation, preliminary bounds on the performance attainable for various uncertainties in malignant tissue properties (permittivity), sizes, location, and signal-to-noise ratios have been obtained.

Body

The details of the research done on this project during this reporting period are summarized below in which the detailed descriptions are cited, References [1-3]. Copies of the conference papers and posters cited [1-3] are included in the appendix of this report.

Background -- Most of the past research in this field has focused on the study of the dielectric properties, the design of the microwave imaging prototypes, and the improvement of the EM forward and inverse algorithms. However, none of this research has incorporated signal detection theory directly into the microwave imaging at the measurement level. Markov Random Fields and detection theory have been applied in mammography for diagnosis. However these only assumed a simple deterministic disk object model or did not utilize the *a priori* knowledge of the projections. This research presents Bayesian algorithms for Scattered Electromagnetic fields through an Uncertain Permittivity Image which incorporates the knowledge of the *a prior* permittivity image modeled by the MRF, the measurement noise, as well as the physical model of the forward scattered electric field. The Bayesian algorithms for the Uncertain Permittivity Image and the Threshold Image Processors are also presented for comparisons. Our approach exploits the propagation of the scattered microwave fields to develop better

diagnostic decision aids. Additional references to this background information are contained in Ref. 2

On this concept research award, Sha, the graduate student on this project, with the help of two other students, has compiled results from experiments in the literature that show that the microwave dielectric properties of malignant tissue is different from that of normal breast tissue [1]. Hence microwave imaging has the potential of providing a tool for improving the diagnosis of breast cancer with no known radiation dangers [1].

Also, on this project, statistical models of tissue characteristics that model simple uncertainties in the tissue permittivity within the framework of microwave imaging are being developed [2, 3]. The Markov Random Field is used to model the breast permittivity cross section as a propagating medium, and incorporate it into the forward Electromagnetic (EM) propagation to predict the random field of the EM measurements at a received array of sensors. These models of tissue permittivity are then incorporated into an optimal signal detection theory framework in which task-oriented goals such as detection and localization of a tumor drive the information processing [2, 3]. Given these EM field measurements, Bayesian approaches are then developed to compute the likelihood ratio for tumor detection and the *a posteriori* probability display of tumor localization. Using the ROC (receiver operating characteristics) as a quantitative performance measure and optimum signal detection theory, initial ROC's have been obtained using the optimum detection and localization information processing methods derived in the above [2,3]. These results provide an upper bound on the detection of the presence or absence of a tumor as a function of tumor permittivity contrast, size, noise, and local spatial permittivity uncertainties that characterize the tissue in microwave imaging [2, 3]. Using PCL (probability of correct localization) as a quantitative measure of how well one can determine the location of a tumor, initial PCL curves have been obtained that provide an upper bound on locating a tumor as a function of tumor contrast [2,3].

Details of this research supported by this project are presented in the conference papers and poster sessions, references [1-3], with copies of drafts of these references [1-3] included in the appendix.

Key Research Accomplishments

- Sha et al have compiled results from experiments in the literature that show that the microwave dielectric properties of malignant tissue is different from that of normal breast tissue, and hence microwave imaging has the potential of providing a tool for improving the diagnosis of breast cancer with no known radiation dangers.

- Developed initial statistical models of tissue characteristics that model simple uncertainties in the tissue permittivity within the framework of microwave imaging.

- Incorporated the models of tissue permittivity developed above into an optimal signal detection theory framework in which task-oriented goals such as detection and localization of a tumor drive the information processing.

- Using the ROC (receiver operating characteristics) as a quantitative performance measure and optimum signal detection theory, initial ROC's have been obtained using the optimum detection and localization information processing methods derived in the above. These results provide an upper bound on the detection of the presence or absence of a tumor as a function of tumor permittivity contrast, size, noise, and local spatial permittivity uncertainties that characterize the tissue in microwave imaging.

- Using PCL (probability of correct localization) as a quantitative measure of how well one can determine the location of a tumor, initial PCL curves have been obtained that provide an upper bound on locating a tumor as a function of tumor contrast

Reportable Outcomes

Liewei Sha, Erika Ward , and Brandon Story ,"A review of dielectric properties of normal and malignant breast tissue," Proceedings of the IEEE SoutheastCon 2002, pp. 457 -462, Columbia, South Carolina, April 5 - 7, 2002.

Liewei Sha, Loren W. Nolte, Zhong Qing Zhang and Qing H. Liu, "Performance analysis for Bayesian microwave imaging in decision aided breast tumor diagnosis," Proceedings of the 2002 IEEE International Symposium on Biomedical Imaging Washington D.C., pp. 1039-1042, Washington, DC, July7-10, 2002.

Liewei Sha and Loren W. Nolte, " Computer-aided algorithms for breast tumor diagnosis using microwave diffraction measurements", Era of Hope 2002 Department of Defense Breast Cancer Research Meeting, Orlando, Florida, September 25-28, 2002.

Conclusions

The initial detection and localization performance results (ROC's and PCL's) show that the decision-aided Bayesian microwave imaging approach proposed in this paper has the potential of providing additional and useful information for radiologists. This Bayesian microwave imaging approach is driven by the ultimate decision tasks of whether or not a tumor is present, and if so where is it. It benefits from incorporating the *a priori* knowledge, although uncertain, of normal and malignant breast permittivity. This approach also gains a decision performance advantage by processing the measurements

directly using signal detection theory, rather than post processing the reconstructed image where some of the information needed for the decision has been lost.

References

Liewei Sha, Erika Ward , and Brandon Story ,"A review of dielectric properties of normal and malignant breast tissue," Proceedings of the IEEE SoutheastCon 2002, pp. 457 -462, Columbia, South Carolina, April 5 - 7, 2002.

Liewei Sha, Loren W. Nolte, Zhong Qing Zhang and Qing H. Liu, "Performance analysis for Bayesian microwave imaging in decision aided breast tumor diagnosis," Proceedings of the 2002 IEEE International Symposium on Biomedical Imaging Washington D.C., pp. 1039-1042, Washington, DC, July7-10, 2002.

Liewei Sha and Loren W. Nolte, " Computer-aided algorithms for breast tumor diagnosis using microwave diffraction measurements", Era of Hope 2002 Department of Defense Breast Cancer Research Meeting, Orlando, Florida, September 25-28, 2002.

Appendices

Author and titles of copies of papers or posters resulting from this research that provide details for body of the report.

1..Copy of the paper by Liewei Sha, Erika Ward , and Brandon Story ,"A review of dielectric properties of normal and malignant breast tissue," Proceedings of the IEEE SoutheastCon 2002, pp. 457 -462, Columbia, South Carolina, April 5 - 7, 2002.

2. Copy of the paper by Liewei Sha, Loren W. Nolte, Zhong Qing Zhang and Qing H. Liu, "Performance analysis for Bayesian microwave imaging in decision aided breast tumor diagnosis," Proceedings of the 2002 IEEE International Symposium on Biomedical Imaging Washington D.C., pp. 1039-1042, Washington, DC, July7-10, 2002.

3. Copy of the paper by Liewei Sha and Loren W. Nolte, " Computer-aided algorithms for breast tumor diagnosis using microwave diffraction measurements", Era of Hope 2002 Department of Defense Breast Cancer Research Meeting, Orlando, Florida, September 25-28, 2002.

Reference 1 Proceedings of the IEEE SoutheastCon, April 5-7, 2002

A Review of Dielectric Properties of Normal and Malignant Breast Tissue

Liewei Sha, Erika Renee Ward and Brandon Stroy
ECE department, Duke University, Durham, NC27708-90291, ls@ee.duke.edu

Keywords: dielectric properties, breast tissue, normal, malignant

ABSTRACT

This paper presents a review of the dielectric properties of normal and malignant breast tissues for radio through microwave frequencies, as well as a brief summary of the experiment methods and the mechanisms that explain the difference in the dielectric properties of normal and malignant breast tissue. This information provides a basis for the development of diagnostic techniques for breast cancer and also highlights the areas that are in need of more experiments.

1. INTRODUCTION

The contrast in the dielectric properties between normal and malignant tissues is a basis for diagnostic applications using microwave devices. The study of normal tissues has been widely reviewed. This paper, in addition, collects together dielectric property data on benign and malignant breast tissues from a number of researchers, and presents them in graphical form so that this information is convenient for general reference. It should be emphasized that the data shown has been interpolated, extrapolated or computed from the graphs and tables, so it is not necessarily precise. This paper also reviews the mechanisms behind the differences in dielectric properties of normal and malignant breast tissues.

Most data are represented in terms of conductivity σ and relative permittivity ε', since σ and ε' of biological materials are practically independent of frequency up to the microwave range [1]. For the two low frequency cases with no σ and ε' available, the data are represented in terms of a parallel combination of a conductance G and a capacitance C. The two pairs of terms are equivalent in that,

$$Y^* = G + j\omega C = (A/d)(\sigma + j\omega\varepsilon_0\varepsilon') \quad (1)$$

Where, Y^* is the complex admittance of the equivalent circuit of an idealized parallel plate capacitor filled with the tissue of σ and ε'. A/d is the geometry factor. We assume (ε',σ) follow a bi-variate normal distribution. Therefore, the modeling of the data can be represented by the specific cross section of the distribution function, which satisfies,

$$\{(x-m_x)^2/\sigma_x^2+(y-m_y)^2/\sigma_y^2-2\rho(x-m_x)(y-m_y)/\sigma_x\sigma_y\}/(1-\rho^2)=1 \quad (2)$$

where, x is the relative permittivity, y is the conductivity, and m_x, m_y and σ_x, σ_y are the marginal mean and variance. ρ is the correlation coefficient of ε' and σ. If only the mean and variance values are available but not the original data pairs, we assume an independent distribution of (ε',σ) and $\rho=0$.

All data are from human breast tissue, except for one case from rats. The category of breast tissues in the literature is ambiguous. In this paper, we define the following major categories of breast tissue.

- fat
- normal, includes glands tissue (lobules that produce milk), and connective tissue (fibrous tissue that surrounds the lobules and ducts)
- benign, includes fibroadenoma and mastitis
- malignant, i.e. breast carcinomas

We first display the data in the low and high frequency regions, in the order of their publication date. Then we discuss the consistency and inconsistency in the data as well as the diagnostic value of the dielectric properties from the data. Finally the mechanisms are reviewed.

2. REVIEW OF EXPERIMENT DATA

2.1. List of data at low frequency

1. Fricke et.al. ([2], 1926, 20kHz, 24°C), measured the parallel capacitance and resistance (R=1/G) of excised samples from 55 patients, using a wheatstone bridge. Several types of tissue were studied: fat, gland, mastitis, fibroadenoma and carcinoma. Data is displayed in Fig.1. Only one sample of fat is measured, no variance is available for this type.

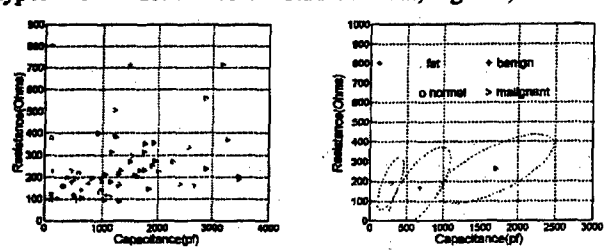

Figure 1: Capacitor versus Resistor
Left: original data; right: modeling of the data

2. Morimoto et.al. ([3,4],1990, 10kHz, 37°C) obtained in vivo measurements of breast cancer, fibroadenoma, normal breast

tissue and fatty tissue using a three-electrode method. The proposed equivalent circuit is composed of R_e parallel with the series of R_i and C_m. We transformed it to parallel R and C, using $R=R_iR_e/(R_i+R_e)$, $C=C_m$. With no original data and correlation coefficient available, Fig.2 displays the modeling of the data, assuming $\rho=0$.

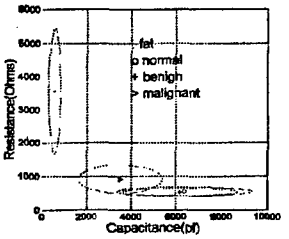

Figure 2: Capacitor versus Resistor

3. Jossinet et.al. ([5,6], 1996, 488Hz-1MHz, 21°C) measured 120 samples from 64 patients, using impedance probe sensors connected with a microcomputer system. In Fig.3, data of six types of tissue is displayed, gland (o), connective (*), fat (•), mastopathy (square), fibroadenoma (+), carcinoma (V). We calculated the relative permittivity and conductivity from the original complex impedance data ρ^* (not the characteristic impedance) using,

$$\varepsilon' = \mathrm{Im}\,(1/\rho^*)/(\omega\varepsilon_0),\ \sigma = \mathrm{Re}(1/\rho^*),\quad \rho^*=1/(\sigma+j\omega\varepsilon_0\varepsilon') \tag{3}$$

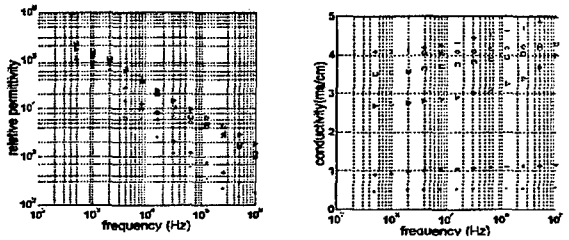

Figure 3 Permittivity and conductivity versus frequency

2.2. List of data at high frequnecy

4. T.S. England et.al. ([7,8], 1949-50, 3-24GHz, 37°) measured the attenuation α nepers/cm, and phase constant β radians/cm of the standing wave pattern of the excised human breast fat and carcinoma tissue samples in the wave-guide. We computed the relative permittivity ε' and conductivity σ using [23, Eqn4.28],

$$\varepsilon=-(\alpha^2-\beta^2)/\omega^2\mu_0\varepsilon_0,\quad \sigma=2\alpha\beta/\omega\mu_0 \tag{4}$$

The variance due to these measurements were computed and presented with the light marker in Fig. 4. Our extrapolations are shown with dashed lines.

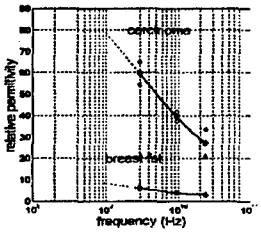

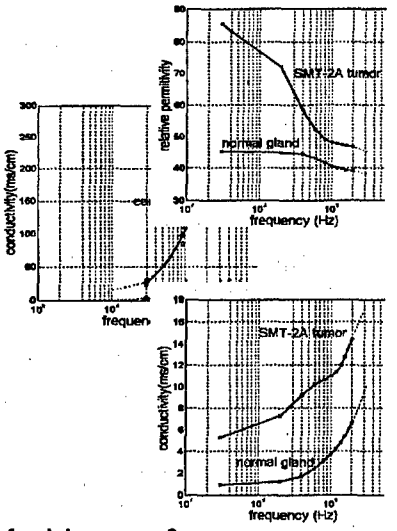

Figure 4 permittivity and conductivity versus frequency

5. W.T. Joines et.al. ([9,10,11], 1980, 30MHz-2GHz, 37°C), obtained in vivo measurements of SMT-2A tumor and mammary gland tissue samples from 22 rats. The nondestructive method uses an open-ended coaxial probe to produce a fringing field in the termination tissue and a directional coupler and an oscilloscope to detect the fringing pattern. The dielectric properties are then computed. The data is shown in Fig. 5, in which skin effect is not corrected, and the data can not be compared with in vitro data directly.

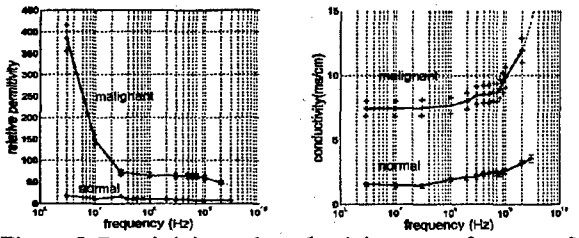

Figure 5: Permittivity and conductivity versus frequency [9]

6. S.S. Chaudhary et.al. ([12], 1984, 3MHz-3GHz, 24°), measured excised normal and malignant breast tissues from 15 patients, using the time domain spectroscopy system of HP. We use the total spread over the mean value (0.8%) to compute the variance of the data, which is shown in Fig. 6.

Figure 6: Permittivity and conductivity versus frequency [12]

7. A.J. Surowiec at.el. ([13], 1988, 0.02MHz-100MHz, 37°) measured the input reflection coefficient of 28 samples from 7 patients, using a coaxial line sensor connected to an HP3577 network analyzer. Tissue types include ductal carcinoma, lobular carcinoma, and surrounding tissues. The measured dielectric values are available only at 100kHz and 100MHz, and we use square symbols to represent the mean and mean±std values of those data in Fig. 7. The authors provided the parameters ε_∞, ε_s, τ, σ_s and α, by fitting the data with the Cole-Cole equations [1],

$$\varepsilon^*=\varepsilon_\infty+(\varepsilon_s-\varepsilon_\infty)/(1+(jf/f_c)^{1-\alpha})-j\sigma_s/\omega\varepsilon_0 \tag{5}$$

where $f_c=1/2\pi\tau$, τ is the relaxation time, f_c is the relaxation frequency, α is the distribution parameter that reflects the

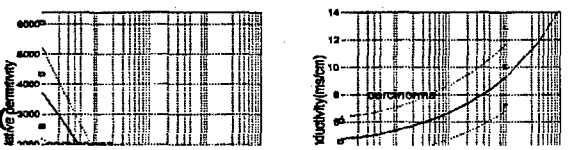

range of τ. s represents the low frequencies $f << f_c$, ∞ represents the high frequencies $f >> f_c$. When α =0, Eqn.5 is the same as Debye equation.

Figure 7 Permittivity and conductivity versus frequency

The curves in Fig. 7 are computed from the fitted Cole-Cole model in [13]. The dark lines are the mean values, the light lines are the mean±std values. Extrapolations are shown in light color. Comparing the mean from the measurements and the model, the conductivity values agree well, but the relative permittivity values show some inconsistency.

8. A.M. Campbell et.al. ([14], 1992, 3.2GHz, 24°C) measured 39 samples of normal breast fat, 18 samples of benign tumors, 22 samples of glandular connective tissue and 20 samples of cancer from 37 patients, using a resonant cavity perturbation method. Dielectric properties were measured using the observation of the changes in resonant frequency. In Fig.8, the left plot displays the original data. The right plot illustrates the modeling of the data with Eqn.2.

Figure 8 conductivity versus permittivity

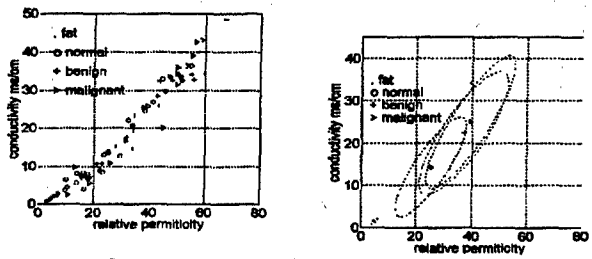

Left: original data; Right: modeling of the data

9. W.T. Joines et al. ([15], 1994, 50MHz-900MHz, 24°C), measured admittance of 12 normal mammary samples and 12 malignant mammary samples from 12 patients, using a flat-ended coaxial probe connected to a network analyzer HP 8754A. ε' and σ are then computed from the admittance with the knowledge of the geometry factor. In Fig. 9, the mean values are presented with the solid lines, the standard error on the mean is presented with the dashed lines. Extrapolations are represented with light lines.

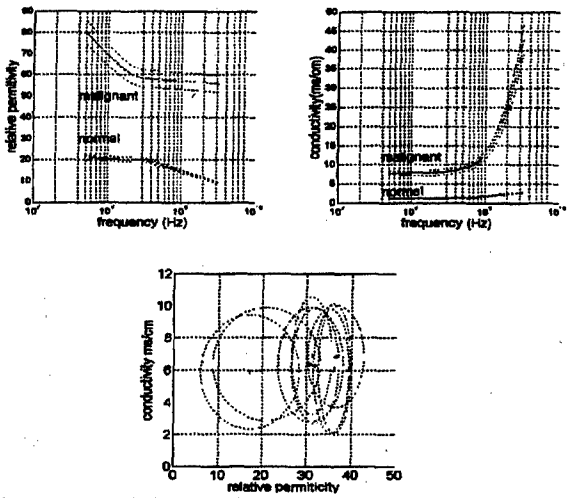

Figure 9 Permittivity and conductivity versus frequencies [15]

10. P.M. Meaney et.al. ([16], 2000 900MHz,37°) obtained the in vivo breast microwave imaging of 5 patients, all non-malignant, at 900MHz.

Figure 10 conductivity versus permittivity

We display the modeling of the data of individuals in Fig. 10 to represent the heterogeneity within and across patients. The correlation coefficient is not available and assumed to be 0.

2.3. Data consistency and inconsistency

Low frequencies. At low frequency ranges, the dielectric values of the four types of tissue are all available for the first three cases, as shown in Figures 1, 2 and 3. We cannot compare them directly, because of the unknown geometry factors in cases 1 and 2. Yet we can still make comparisons according to the relative distribution of the data for the same tissue types. The consistencies noted are listed below,

- The conductivity of the malignant tissue falls between the fat (plus connective tissue) and the normal gland tissue (plus the benign fibroadenoma and mastitis tissues).
- The benign and normal tissues can be grouped together relative to the malignant tissues on the ε'-σ plane.
- The relative position of the fat tissue on the ε'-σ plane compared to the other types is the same.

This information of data consistency provides a basis for identifying breast cancer, benign tumor and normal breast tissue using the tissue conductivity at 1kHz-1MHz.

The inconsistency in the first three cases is that the malignant tissue has lower capacitance (or permittivity) than that of the normal and benign tissues in case 2 and the lower frequency region of case 3, but it has the largest capacitance values in cases 1 and the higher frequency region of case3. One of the possible reasons for the inconsistency is the frequency difference. It is 10kHz in case 2, 20kHz in case 1 and 488Hz–1MHz in case 3. Therefore, the inconsistency can be related with a turning frequency point in tens of kHz, above which the capacitance value of cancerous tissues became larger than that of normal and benign tissues. Other reasons for the inconsistency are the intrinsic heterogeneity and the temperature difference of tissue samples.

This information of inconsistency suggests that in the range 1kHz to 1MHz, the capacitance of breast tissues is not a good quantity to diagnose breast cancer. More experiments and analyses on the capacitance properties of normal and malignant breast tissues are needed in this frequency range.

High frequencies. In the high frequency range, we can compare the dielectric data directly.

Figure 11 Permittivity versus frequency

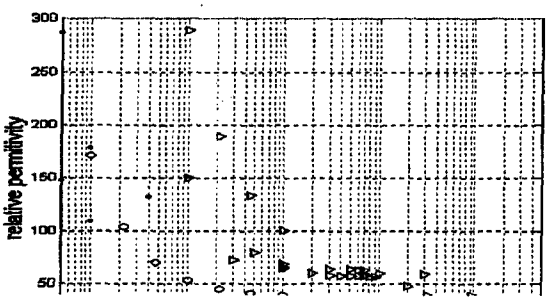

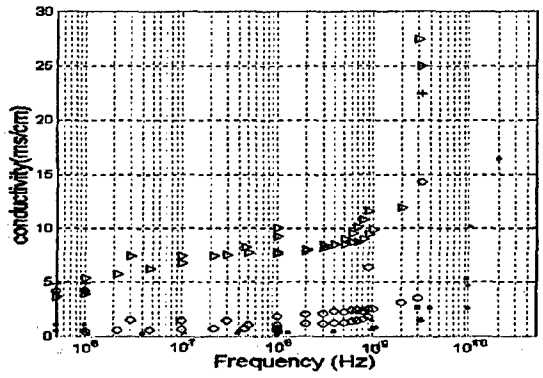

Figure 12 Conductivity versus frequency

Fig. 11 and 12 illustrate the dielectric data together in the range 500KHz to 20GHz. One more case of breast fat [21] is included. Four types of breast tissue: fat (•), normal (o), benigh (+), malignant (∇) are displayed.

For a clearer view, Fig. 13 and 14 illustrate the modeling of the data for multiple cases on the ε'-σ plane at 900MHz and 3.2GHz. Again, four types of breast tissue: fat (•), normal (o), benign (+), malignant (∇) are displayed.

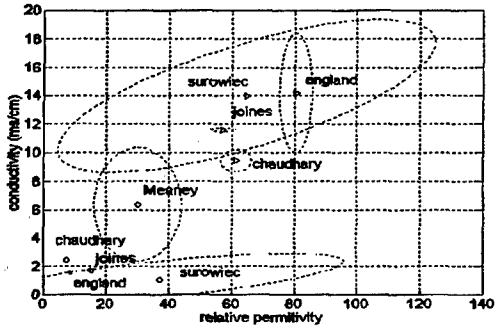

Figure 13 Conductivity versus Permittivity, at 900MHz

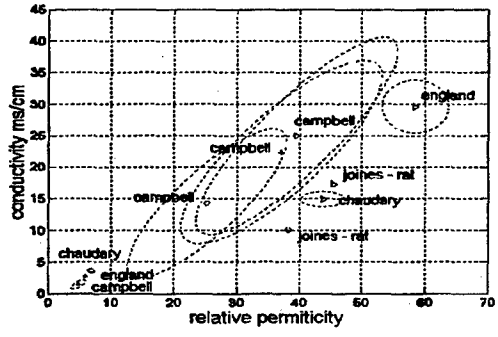

Figure 14 Conductivity versus Permittivity, at 3.2GHz

From Fig. 11-14, we observe the data inconsistency,

- The mean dielectric values of normal and malignant breast tissues have obvious variability.
- The mean conductivity values of normal breast tissues in Joines' rat data, Campbell's data, and Meaney's data are more than twice that of other normal breast tissue cases at the corresponding frequencies. The mean permittivity values of normal breast tissue in Joines' rat data and Campbell's data are more than twice that in England's data and Chaudhary's data at 3.2GHz frequency.

The possible two reasons for the inconsistency are listed below, which may help explain the results and improve the future experiment designs.

- Experiment method
  1. Limitations in experiments. Chaudhary's samples were collected in physiological saline, which will affect the accuracy of the data. Campbell's malignant samples are frozen and defrosted before the measurement, which may affect the accuracy of the data of this type.
  2. In vivo vs in vitro. Joines' rat data is from in vivo measurements with uncorrected skin effects. Meaney's data comes from reconstruction of in vivo microwave imaging. Others are from excised samples. In vivo methods seem to have higher dielectric values.
  3. Sample temperature differences. Lower sample temperature will make the dielectric value a little bit lower, when the frequency is below 2GHz.
- Intrinsic heterogeneity
  1. Normal breast tissues are composed of breast fat, connective tissue and gland tissue, etc. In the literature, the composition of normal breast tissues from case to case may differ.
  2. Different stages of tumor development will change the tumor's dielectric property and introduce variability [2,13]. Some samples of malignant tissues were actually composed of small parts of malignant cells infiltrating within a large part of normal cells, which may decrease the mean value of the malignant tissue samples.
  3. Across patients. The breast tissue samples from patients with different water content or fat content and in different stage of menstruation, pregnancy or lactation will have obvious differences in dielectric values. Campbell's data came from a relatively larger patient group, which may introduce wider variability.

This inconsistency information indicates the importance of using proper sample storage method before experiments and suggests a standardization of the experiment conditions like the sample and environment temperatures, as well as the record of patients' information for later analysis.

Although there are so many conditions out of control, we still observe the data consistency from Fig. 11-14

- The mean conductivity of the normal tissue is less than 15ms/cm up to 3.2GHz.
- Malignant tissues have higher mean permittivity and conductivity values than those of normal breast tissues
- Fat tissues have the lowest mean permittivity and conductivity values

This data consistency information provides the basis for breast cancer diagnosis using the dielectric properties in the microwave frequency range.

2.4. Discussion of the diagnostic values

It is misleading to use only the contrast of the mean values to judge the diagnostic value of the dielectric properties. Since the intrinsic heterogeneity in malignant tissue is large, this will decrease the mean contrast. The mean values from samples across patients will decrease the contrast as compared to an individual patient. Therefore, the diagnostic value of the dielectric properties seems to be underestimated, as in case 8. A better concept might be to use the contrast of the maximum value of the malignant tissue with the mean of the neighborhood normal tissue samples [2,13]. Better criterion can be defined using the probability of detection and false alarm, in which the random model of the point dielectric values and the spatially distributed dielectric values are incorporated.

In summary, we observed the diagnostic value of the dielectric properties from the data, as

- The low conductivity values of the normal breast tissue enable penetration of microwave frequencies up to the low GHz range, which coincides with the simulation results in [22].
- At 100MHz-1GHz, dielectric properties can significantly help classify normal and malignant tissues.
- At frequency ranges of 1GHz-3GHz, dielectric properties can help classify normal and malignant tissues.
- At 10kHz-1MHz, dielectric property can help classify normal, benign and malignant tissues, yet mainly depends on the conductivity.

2.5. Areas in need of more experiments

- The dielectric properties of benign tissues compared with that of the malignant tissues and normal tissues in the frequency range of 100MHz-3GHz.
- The spatial distribution of the dielectric properties of normal, benign and malignant breast tissues.
- The dielectric properties of human breast cancer in different development stages.

3. MECHANISM: NORMAL VS MALIGNANT TISSUE

We first review the mechanism of the dielectric properties of biological tissues in general.

The frequency dependence of dielectric properties of biological tissues is related to the polarization of molecules and structural interfaces in response to the applied electric field [9]. Data from Schwan and Foster on high water content muscle tissue suggests the presence of three dispersion regions: alpha, beta, and gamma, with the relaxation frequencies to be kHz, hundreds of kHz, and GHz [17]. The delta dispersion, located in half way between beta and gamma regions, has also been identified [1,18,19].

For engineering applications, the alpha dispersion has little significance [1]. Beta dispersion occurs at radio frequencies, and arises principally from the charging of cellular membranes, with smaller contributions from the protein constituents and ionic diffusion along surfaces in the tissue [1,18,19].

Tissues typically exhibit a small dispersion between 0.1 and 3GHz, which have been termed the delta dispersion [1,19] or "UHF relaxation" [18]. A combination of mechanisms are suggested for this region: bipolar relaxation of the water of hydration "bound" to proteins, a Maxwell-Wager effect due to ions in the cytopalsm collection against relative nonconductive protein surface and rotation of polar side-chains on the protein surface [1,9,18]. The relaxation frequency is dominant mostly by bound water (fr of 100-1000 MHz [1], Protein molecules (fr of 40-300 MHz) and free water (fr=25GHz).

The gamma dispersion occurs with a center frequency near 25GHz at body temperature, due to the dipolar relaxation of the free and bound water and ionic conductivity. Campbell and Land [14] attribute higher than expected conductivity at 3.2 GHz to the "tail end" of β-dispersion effects.

In recent studies, a variety of factors have been explored, which lead to pronounced difference in dielectric properties in normal compared with malignant tissues, as listed below:

Necrosis. Inflammation and necrosis are commonly found in malignant breast tissues. Presence of necrosis leads to breakdown of cell membranes and thus a larger fraction of the tissue that can carry current at low frequencies [20], which decreases the capacitance of the tumor [2].

Charging of the cell membrane. In breast carcinoma, there is a progressive replacement of fat lobules with fibroblastic proliferation and epithelial cells. Which also accompanied by a variety of alterations at the transformed cell surface [12(22)]. Cancer cells have reduced membrane potentials and tend to have altered ability to absorb positive ions [19(77)], they have a higher negative surface charge on their membranes [9(4,21),19(78)]. According to Joines et.al., conductivity of the malignant tissues is increased with this mobile charge being displaced and rotated by the microwave field [9].

Relaxation times. The relaxation times in malignant tissues are larger than those in normal tissue, indicating that a significant increase in the motional freedom of water has occurred [19(75)]. Surowiec et.al.[13] reported that cancerous breast tissues have average dielectric relaxation times between 0.6us and 1.4 us and the surrounding normal tissues had shorter relaxation times of 0.3us.

Sodium concentration and water content. The sodium concentration in tumor cells is higher than in normal cells [19(76)]. The excessive sodium concentrations not only affect the cell membrane potentials [10, (9-11)], but causes malignant tissue to retain more fluid. According to Joines et.al, the excess sodium fluid alone would yield greater conductivity and permittivity values in malignant tissue than in normal tissue. In addition, the fluid is retained in the form

of bound water, which has larger values of σ and ε than free water [10].

Malignant tissues have significantly higher water contents than normal tissues [18,19 (76)]. The data from Campbell and Land [14] illustrates the dielectric properties related with the water content at 3.2GHz of the breast tissues, as shown in Fig. 15 and 16. The relationship between relative permittivity and water content is strikingly similar to the relationship between conductivity and water content. This leads to the conclusion that the same mechanism is responsible for the change in both dielectric properties.

Malignant breast tissue has a higher ratio of water content compared with that of the normal tissue, which coincides its higher values of permittivity and conductivity than normal breast tissue at the same microwave frequency. However, in this data taken at 3.2 GHz, there is not a marked difference in the water content of benign breast tissue and malignant tumor.

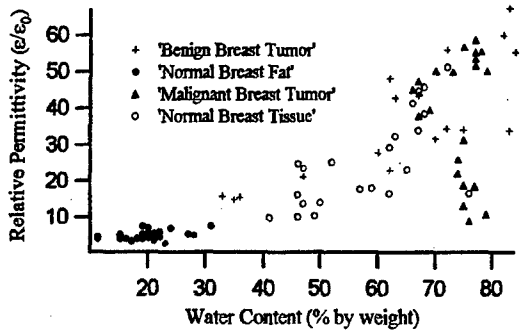

Figure 15 Relative permittivity of human breast tissue vs water content

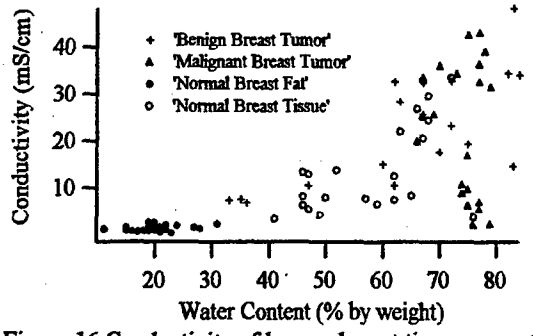

Figure 16 Conductivity of human breast tissue vs. water content

4. CONCLUSION

This paper presents an initial review and consolidation of the dielectric properties of normal, benign and malignant tissues in the range of 10kHz-20GHz. A brief explanation of the experiment methods is presented as well as the mechanisms that explain the difference in the dielectric properties of normal and malignant tissues. The consistency and inconsistency of the data are discussed as well as suggestions for the possible inconsistency. It is observed that the dielectric properties of breast tissue, even though containing uncertainty, have good diagnostic value in the range of 100MHz-3GHz.

ACKNOWLEDGEMENT

I appreciate Dr. Loren W. Nolte and Dr. William T. Joines's help of modifying this paper and I wish to thank Dr. Gary Ybarra and Dr. Qing H. Liu for their helpful discussions. This work was supported in part by NIH/NCI under grand 5PO1 CA42745-13.

REFERENCES

1. K.R. Foster and H.P. Schwan, Dielectric properties of tissues in CRC Handbook of Biological Effects of Electromagnetic Field, C. Polk and E. Postow Eds. Boca Raton, CRC Press, 1996
2. H. Fricke and S. Morse, "The Electric Capacity of Tumors of the Breast", *J. Cancer Res.*, vol. 16, pp. 310-376, 1926.
3. Morimoto, T, Kinouchi Y, Iritani T, "Measurement of the electrical bio-impedance of breast tumors". Eur Surg Res. 1990;22:86-92
4. Morimoto, T., Kimura, S. et.al, "A study of the electrical bio-impedance of tumors", J.Investig. Surg. 1993;6:25-32
5. J. Jossinet, "Variability of impedivity in normal and pathological breast tissue", Med. & Biol.Eng. & Computing 1996;34:346-350
6. J. Jossinet, "The impedivity of freshly excised human breast tissue", Physiol. Meas. 1998;19:61-75
7. T.S. England and N.A. Sharples, "Dielectric Properties of the Human Body in the Microwave Region of the Spectrum Nature March 1949;163:487-488
8. T.S.England, "Dielectric Properties of the Human Body for Wave-lengths in the 1-10 cm Range", Nature Sep. 1950;166:480-481
9. W. T. Joines, R. L. Jirtle, M. D. Rafal, D. J. Schaefer, "Microwave Power Absorption Differences Between Normal and Malignant Tissue", *Int. J. Radiation Oncology Biol. Phys.*, vol. 6, pp. 681-687, 1980.
10. W. T. Joines, "Frequency-Dependent Absorption of Electromagnetic Energy in Biological Tissue", *IEEE Transactions on Biomedical Engineering*, vol. BME-31, no. 1, pp. 17-20, January 1984.
11. E. Tanabe W.T. Joines, "A nondestructive method for measuring the complex permittivity of dielectric materials at microwave frequencies using an open transmission line resonator", IEEE Trans. Instrumentation and Measurements 1976;25:222-226
12. S. S. Chaudhary, R. K. Mishra, Arvind Swarup, Joy M. Thomas, "Dielectric Properties of Normal & Malignant Human Breast Tissues at Radiowave & Microwave Frequencies", *Indian Journal of Biochemistry & Biophysics*, vol. 21, pp. 76-79, February 1984.
13. A.J. Surowiec, S.S Stuchly, J.R. Barr, A. Swarup, "Dielectric Properties of Breast Carcinoma and the Surrounding tissues", IEEE Trans. Biomed. Eng. 1988; Vol 35, No.4:257-263
14. A. M. Campell, D. V. Land, "Dielectric properties of female human breast tissue measured *in vitro* at 3.2 GHz", *Phys. Med. Biol.*, vol. 37, no.1, pp. 193-210, 1992.
15. William T. Joines, Yang Zhang, Chenxing Li, and Randy L. Jirtle, "The measured electrical properties of normal and malignant human tissues from 50 to 900 MHz", *Medical Physics* April 1994;vol 21;4:547-550
16. Paul M. Meaney, Margaret W. Fanning, Dun Li, Steven P. Poplack, and Keith D. Paulsen, "A Clinical Prototype for Active Microwave Imaging of the Breast", *IEEE Transactions on Microwave Theory and 7Techniques*, vol. 48, no. 11, pp. 1841-1853, November 2000.
17. P.Debye *Polar Molecules*. New York, Dover. 1929, pp. 77-108.
18. K.R. Foster, J. L. Schepps, "Dielectric Properties of Tumor and Normal Tissues at Radio through Microwave Frequencies", *Journal of Microwave Power*, vol. 16, no. 2, pp. 107-119, 1981
19. R.Pethig "Dielectric Properties of Biological Materials: Biophysical and Medical applications", IEEE trans. on Electrical Insulation Oct.1984;vol. EI-19 No5:453-472S
20. R.Smith,K.R. Foster and J.L.Wolf, "Dielectric properties of VX-2 carcinoma vs. normal liver tissues", IEEE trans Biomed. Eng., BME-33,522,1986
21. C.Gabriel,S.Gabriel, "Compilation of the Dielectric Properties of Body Tissues at RF and Microwave, Frequencies", http://www.brooks.af.mil/AFRL/HED/hedr/reports/dielec

tric/Title/Title.html
22. J.R. Mallard, D.C. Lawn "Mammary tumor", Nature 1967;213:28-30
23. Constantine A. Balanis, *Advanced Engineering Electromagnetics*, John Wiley & Sons 1989, p146

This research supported in part by AMRMC Grant DAMD17-01-1-0513.

Reference 2 Proceedings of the 2002 IEEE International Symposium on Biomedical Imaging, Washington, DC, July 7-10, 2002

PERFORMANCE ANALYSIS FOR BAYESIAN MICROWAVE IMAGING IN DECISION AIDED BREAST TUMOR DIAGNOSIS

Liewei Sha, Loren W. Nolte, Zhong Qing Zhang, and Qing H. Liu

Dept. of Electrical and Computer Engineering, Duke University
Durham, NC 27708-0291, lwn@ee.duke.edu

ABSTRACT

In this paper the Markov Random Field is used to model the breast permittivity cross section as a propagating medium, and incorporate it into the forward Electromagnetic (EM) propagation to predict the random field of the EM measurements at a received array of sensors. Given these EM field measurements, Bayesian approaches are then developed to compute the likelihood ratio for tumor detection and the *a posteriori* probability display of tumor localization. Quantitative performance evaluations using simulations demonstrate the advantage of using the Bayesian approach to directly process the measurement data as compared to using the Bayesian or threshold approaches to detect and localize the tumor based on the reconstructed permittivity image.

1. INTRODUCTION

Microwave imaging is a promising new modality for breast cancer diagnosis, partly because it is non-invasive and the permittivity contrast between normal and malignant breast tissues is high [1]. In addition, the attenuation of EM propagation in normal breast tissues is low so that it can penetrate into the depth of the tissue [1]. Most of the research in this field has focused on the study of the dielectric properties [1,(1-22)], the design of the microwave imaging prototypes [2], and the improvement of the EM forward and inverse algorithms [3][4][5]. However, none of this research has incorporated signal detection theory directly into the microwave imaging at the measurement level. Markov Random Fields (MRF Hammersley and Clifford [6]) and detection theory have been applied in mammagraphy for diagnosis, such as [7][8][9]. However, [7] and [8] only assumed a simple deterministic disk object model. [9] did not utilize the *a priori* knowledge of the projections. This paper presents Bayesian algorithms for Scattered Electromagnetic fields through an Uncertain Permittivity Image (*BP_SEUPI*), which incorporates the knowledge of the *a prior* permittivity image modeled by the MRF, the measurement noise, as well as the physical model of the forward scattered electric field. The Bayesian algorithms for the Uncertain Permittivity Image (*BP_UPI*) and the Threshold Image Processors (*TIP*) are also presented for comparisons. It should be noted that the forward EM scattering field is computed using the Extended Born Approximation (EBA) accelerated CGFFT method, which has been proposed by Zhang and Liu in [4][10]. The reconstructed permittivity image is obtained using the EBA as the initial solution followed by the Contrast Source Inversion (CSI [11]) method, which has been proposed by Zhang and Liu [4].

2. DIAGNOSIS MODEL

The binary hypotheses considered are:
H_0: No tumor present
H_1: Tumor(size L×L) present, located at an unknown position S on the 2D lattice Ω of the permittivity cross section.

The decision as to whether the tumor is present or not, i.e. whether H_0 or H_1 is true, is the detection problem. Where the tumor is located if H_1 is true, is considered to be a localization problem.

The data for the BP_SEUPI are the microwave measurements r, shown in the middle of the Fig. 1. r is composed of concatenating pieces. Each piece is a complex K×1 vector representing the narrow-band frequency component of the scattered electric field sampled by K sensors, from a single transmitter, which is one of the K sensors. It assumes $r = s + n$, s is the signal, and n is the additive noise at the sensors, modeled by a multivariate complex Gaussian distribution, with zero mean and $\sigma_n^2 I_{K^2}$ covariance matrix. The signal to noise ratio (SNR) is given by $10log10(\frac{\|s\|^2}{\sigma_n^2})$ (dB). The propagating medium of the EM field is the uncertain permittivity image modeled by the MRF, a sample of which is shown in the left of Fig. 1.

The data for BP_UPI and TIP is the reconstructed permittivity image $\epsilon_r = T^{-1}(r)$, as shown in the right of Fig. 1 where T^{-1} represents the reconstruction procedure.

The uncertainties in this problem are the tumor position, the noise at the sensors, as well as the spatial distribution of the breast permittivity which reflects statistically the tissue variance in individuals and the background structure variance across patients.

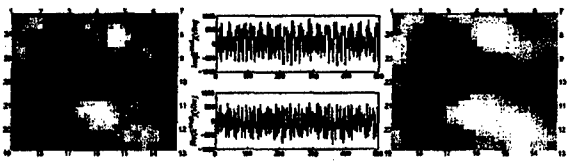

Fig. 1. Numbers 1-24 represent the sensors. Left: original tissue permittivity image; Middle: real and imaginary part of a sample measurement data; Right: reconstructed tissue permittivity image.

2.1. Model of Breast Permittivity Image

We utilize the MRF to model the breast permittivity image, because it implements the idea that spatially nearby tissue permittivities are similar. The Gaussian MRF (GMRF, Chellappa [6]) is selected because it provides a simple form to be incorporated in the Baysian approaches. It is important to realize that this model is statistical, and is not intended to be a model of the detailed deterministic structure of permittivity of a particular individual. The GMRF is defined as

$$p(x_{ij}|x_{kl} \in \Omega \setminus \{(i,j)\}) = \frac{\exp(-\frac{1}{2\sigma_{ij}^2}(x_{ij}-(\mu_{ij}-\sum_{kl\in\mathcal{N}_{ij}}\beta_{(ij),(kl)}(x_{kl}-\mu_{kl})))^2)}{\sqrt{2\pi\sigma_{ij}^2}}, \quad (1)$$

where μ_{ij} and σ_{ij}^2 are the mean and variance at (i,j). $\beta_{(ij),(kl)}$ are the interaction coefficients. The β's provide two kinds of information: one is the neighborhood of (i,j), i.e. $\mathcal{N}_{ij}$ which implies that the permittivity at (i,j) only depends on the permittivities in it's neighborhood. Another is the influence of the neighbors on the point (i,j), as represented by the sign and value of the interaction coefficients.

We assume the permittivity image size is 9.2cm×9.2cm, 529 pixels. The tumor size is 25 pixels. The mean values of tumor and background are $\mu_t = 40$ and $\mu_b = 30$, whose values are similiar to normal and malignant breast permittivity values from experiments [1]. The interaction coefficients of tumor and background are β_t with 3 pixel correlation length and β_b with 20 correlation length. An algorithm proposed by Rue [12] is used to fit the interaction coefficients to the Gaussian field. Applying Hammersley-Clifford theorem [6], given Eqn.1, we derive the mean vector μ and μ_S, covariance matrix Q and Q_S of the joint pdf of the permittivity image under the H_0 and H_1 conditions respectively. Subscript S denotes the tumor position.

2.2. Detection and Localization Approaches

According to signal detection theory, the optimal detector is the likelihood ratio of the data vector followed by a threshold whose value is determined by the optimum criterion (T.G.Birdsall). The optimal localization processor calculates the *a posteriori* probability of the tumor position given the data vector. We derive the likelihood ratios(λ) for the Bayesian detector and threshold detector, as well as the *a posteriori* probability image for the Bayesian localization processors. We assume that the unknown tumor position has a uniform distribution *a priori* on the 2D lattice Ω.

2.2.1. Bayesian Processor for Scattered EM field propagated through theUncertain Permittivity Image (BP_SEUPI)

detector $\lambda(r) \propto$

$$\frac{\sum_{S\in\Omega}\int_{\epsilon_r}\exp(-\frac{(r-T(\epsilon_r))^T(r-T(\epsilon_r))}{2\sigma_n^2})p(\epsilon_r \mid H1,S)d\epsilon_r}{\int_{\epsilon_r}\exp(-\frac{(r-T(\epsilon_r))^T(r-T(\epsilon_r))}{2\sigma_n^2})p(\epsilon_r \mid H0)d\epsilon_r} \quad (2)$$

localization processor

$$p(S|r) \propto \int_{\epsilon_r}\exp(-\frac{(r-T(\epsilon_r))^T(r-T(\epsilon_r))}{2\sigma_n^2})p(\epsilon_r|H1,S)d\epsilon_r. \quad (3)$$

Both the BP_SEUPI detector and the localization processor require a high dimensional integration, which is a tough problem. This paper tries to overcome this difficulty by using a multivariate complex Gaussian distribution to approximate the random field of the measurements data, which has been found to have good performance in the simulations.

2.2.2. Bayesian Processor for Uncertain Permittivity Image (BP_UPI)

detector $\lambda(\epsilon_r) \propto$

$$\sum_{S\in\Omega} \mid Q_S \mid \exp(\frac{(\epsilon_r-\mu)^TQ(\epsilon_r-\mu)-(\epsilon_r-\mu_S)^TQ_S(\epsilon_r-\mu_S)}{2}) \quad (4)$$

localization processor

$$p(S|\epsilon_r) \propto \mid Q_S \mid \exp(-\frac{(\epsilon_r-\mu_S)^TQ_S(\epsilon_r-\mu_S)}{2}) \quad (5)$$

2.2.3. Threshold Image Processor(TIP)

detector $\lambda = max \ \ \epsilon_r$ (7)

localization processor $S = \underset{S\in\Omega}{max}\ \epsilon_r(S)$ (8)

3. SIMULATION RESULTS

3.1. An example

Fig. 2a) shows an example of a stochastic background permittivity image of the tissue, along with a simulated tumor, modeled by the GMRF. Fig. 2b)-d) are the reconstructed permittivity images from the perfect measurement data as well as from 60dB and 50dB noisy measurement data. The

signal detection approach using the permittivity data computes the *a posteriori* probability of the tumor location given either the original permittivity image, or the reconstructed image as data. Fig. 2e gives an upper bound on tumor localization by plotting the *a posteriori* probability of tumor location using the tissue data of Fig. 2a. Fig. 2f-h shows the *a posteriori* plots of tumor location based on post processing the reconstructed tissue data shown in Fig. 2b-d. Fig. 2j-l shows the *a posteriori* plot of tumor location based on the same measurements used to get the reconstructions in Fig. 2b-d.

Plots 2g-h show that at the 60dB and 50dB SNR condition, the BP_UPI using the reconstructed data misses the correct location of the tumor, and Fig. 2k-l shows that the BP_SEUPI using the measurement data gets the correct tumor localization with high probability. This is a specific example where the BP_SEUPI works better. In the following sections, it is demonstrated statistically that the processors using the measurement data have better performance.

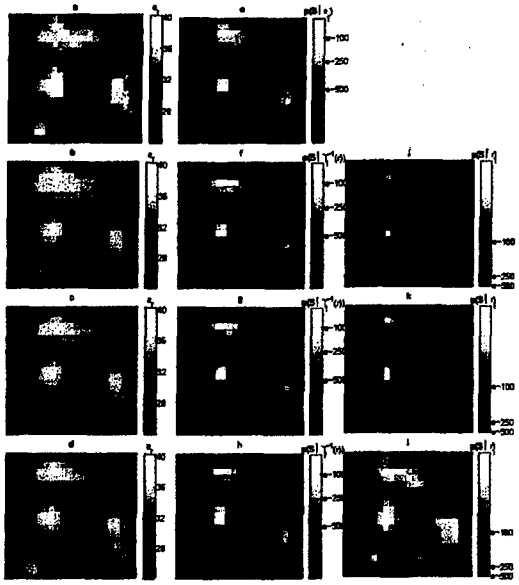

Fig. 2. a) Original tissue permittivity image; b)-d) Reconstructed permittivity from the measurement data b) without additive noise c)d) with additive noise, c) 60dB SNR d) 50dB SNR; e)-h) the *a posteriori* probability of the tumor position given the permittivity image data - $p(S \mid \epsilon_r)$, data ϵ_r comes from a)-d); j)-l) the *a posteriori* probability of the tumor position given the measurement data - $p(S \mid r)$

3.2. Detection performance

Fig. 3a) illustrates the detection performance comparisons assuming no additive noise. In 3a) the ROC of the threshold detector provides a performance lower bound. The TIP mimics the way a routine visual examination of the image might be done. Although it is not sophisticated, it's ROC reflects the problem of high positive predictive Value(PPV) of conventional mammography. Using the reconstructed permittivity image data, the BP_UPI detector is much better than the TIP detector, especially when the probability of false alarm is low, because the BP_UPI utilizes the *a priori* knowledge of the tissue background across patients and the *a prior* knowledge of the different characteristics of the normal and malignant tissues to improve the detection performance.

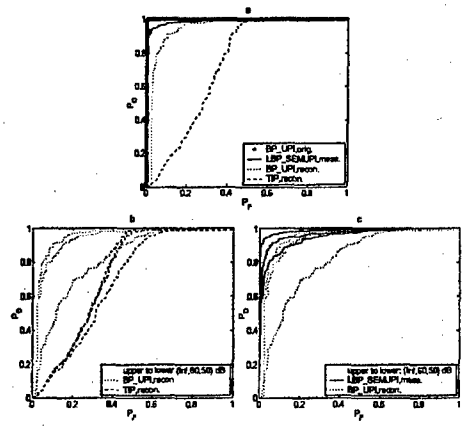

Fig. 3. The detection performance of the BP_UPI using original tissue data, BP_UPI using reconstructed permittivity image data, TIP using reconstructed permittivity image data and BP_SEUPI using measurement data. a)no additive noise presents at sensors; b)c) [Inf, 60,50] dB noise at sensors b) BP_UPI & TIP c) BP_UPI & BP_SEUPI

Fig. 3a) also shows that the BP_SEUPI detector using the measurement data is better than BP_UPI detector using the reconstructed permittivity data, yet worse than BP_UPI detector using the original permittivity data. In reality, we do not have access to the original tissue permittivity image directly but to the EM measurements. However, this provides an upper bound for performance evaluations. The BP_UPI detector using the original permittivity data is better than the BP_SEUPI because the forward EM field maps the variables from the original permittivity domain to the measurement domain, which shrinks the random variable space and decreases the detectablity.

Fig. 3b)c) compares the performance of the detectors when noise is present. It indicates that sensor noise degrades all the detection performances. It also demonstrates that for three SNR conditions, both Bayesian detectors are better than the threshold detector and the BP_SEUPI is better than the BP_UPI using the reconstructed permittivity data.

3.3. Localization performance

Fig. 4 shows the localization performance of the BP_SEUPI using the measurement data, and the BP_UPI and TIP using the reconstructed tissue permittivity data. The localization

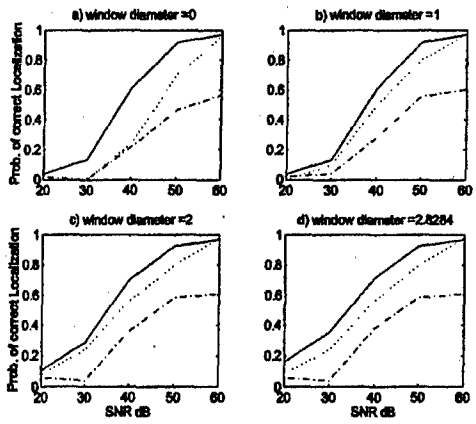

Fig. 4. Localization performances: solid line, BP_SEUPI using the measurement data; dotted line, BP_UPI using the reconstructed tissue permittivity data; dashed line, TIP using the reconstructed tissue permittivity data

performance is shown using the probability of correct localization (PCL) curves. PCL is obtained by computing the ratio of the number of correct localizations over the total trials. The localization is correct if the located tumor position is within the test window. If it is required that the located position is exactly the same as the real position to be true, the window diameter is zero. For the other values of the window diameter:1,2,2.8284, the window sizes are 9,13,25 pixels. Fig. 4 shows that at 50dB or 60dB SNR condition, both the BP_UPI and the BP_SEUPI have better performance than 0.9 PCL. They are much better than the threshold approach for all the tested SNR conditions. The BP_SEUPI localization using the measurement data is the best of the three.

4. CONCLUSION

The results of the detection and localization performances show that the decision-aided Bayesian microwave imaging approach proposed in this paper, BP_SEUPI, has the potential of providing additional and useful information for radiologists. It is an algorithm whose goal is at the heart of the ultimate decisions; i.e. is a tumor present, and if so where. It benefits from incorporating the *a priori* knowledge, although uncertain, of normal and malignant breast permittivity. It also gains a decision performance advantage by processing the measurements directly rather than as a post processor to a reconstructed image.

5. REFERENCES

[1] Liewei Sha and Erika R. Ward etc, "A review of dielectric properties of normal and malignant breast tissue," *Accepted by IEEE SoutheastCon2002, April.*

[2] P. M. Meaney and K. D. Paulsen etc, "A clinical prototype for active microwave imaging of the breast," *IEEE Transactions on Microwave Theory and Techniques*, vol. 48, no. 11, pp. 1841–1853, Nov. 2000.

[3] Q. H. Liu Z. Q. Zhang T. Wang G. Ybarra L.W. Nolte J. A. Bryan W. T. Joines, "Active microwave imaging I: 2-D forward and inverse scattering methods," *IEEE Trans. Microwave Theory Tech.*, vol. 50, no. 1, pp. 123–133, Jan 2002.

[4] Z. Q. Zhang and Q. H. Liu, "Two nonlinear inverse methods for electromagnetic induction measurements," *Geosci. Remote Sensing*, vol. 39, no. 6, pp. 1331–1339, June 2001.

[5] S. C. Hagness A. Taflove etc., "Three-dimensional fdtd analysis of a pulsed microwave confocal system for breast cancer detection: Design of an antenna-array element," *IEEE Trans. Antennas and Propagation*, vol. 47, pp. 783–791, May 1999.

[6] S. Z. Li, *Markov Random Field Modeling in Computer Vision*, Comp. Sci. Workbench. Springer, 1995.

[7] D. J. Rossi and A. S. Willsky, "Reconstruction from projections based on detection and estimation of objects-part i and ii: Performance analysis and robustness analysis," *IEEE Trans. on ASSP*, vol. ASSP-32, no. 4, pp. 886–906, August 1984.

[8] D. Jalihal and L. W. Nolte, "Signal detection theory and reconstruction algorithms - performance for images in noise," *IEEE trans. on Biomedical Engineering*, vol. 41, no. 5, pp. 501–504, May 1994.

[9] H. D. Li M. Kallergi etc., "Markov random field for tumor detection in digital mammography," *IEEE trans. on Medical Imaging*, vol. 14, no. 3, pp. 565, Sep 1995.

[10] Z. Q. Zhang and Q. H. Liu, "Reconstruction of axisymmetric media with an ffht enhanced extended born approximation," *Inverse Problems,invited paper*, vol. 16, no. 5, pp. 1281–1296, 2000.

[11] P. M. Berg and R. E. Kleinman, "A contrast source inversion method," *Inverse Problems*, vol. 13, pp. 1607–1620, 1997.

[12] H. Rue and H. Tjelmeland, "Fitting gaussian markov random fields to gaussian fields," *Statistics,NO.16*, 1999.

Decision Aided Algorithms for Breast Tumor Diagnosis Using Microwave Diffraction Measurements

Liewei Sha, Loren W. Nolte, Zhong Qing Zhang and Qing Huo Liu
Department of Electrical and Computer Engineering, Duke University, Durham, NC

INTRODUCTION

Microwave energy has the advantages that at low power levels there are no radiation dangers, no contrast agents, and the examinations are comfortable. The proposed approach addresses directly the decision-theoretic task of detection and localization of breast tumor, using microwave diffraction measurements. Bayesian detection theory is used to improve the probability of correct detection and localization. This improvement in performance is possible because conventional imaging techniques, by themselves, usually emphasize resolution and contrast, and leave the incorporation of uncertainties and decisions primarily to algorithms or human observers that post process the reconstructed image. This approach augments conventional medical image processing and provides additional processing of the scattered microwave field to aid the radiologist in dealing with uncertainties that are an inherent part of the decisions.

Sha et al have compiled results from experiments in the literature that show that the microwave dielectric properties of malignant tissue are different from those of normal breast tissue. Signal detection theory, in its most fundamental form, provides a framework for incorporating this knowledge of breast tissue characteristics directly into the design of optimal task oriented information processing algorithms to aid in the detection of breast cancer. In addition, signal detection theory enables one to obtain upper limits of detection and localization performance as a function of uncertainties in the microwave properties of breast tissues, using quantitative measures such as the ROC (probability of detection vs. false alarm) and PCL (probability of correct localization). The proposed algorithm uses the direct microwave diffraction measurements[1] and incorporates the fact that spatially adjacent tissues are similar in their permittivity values, but normal and malignant breast tissues have high contrast in the mean.

Using the ROC and PCL performance measures and simulations, the best tumor detection and localization performance for microwave imaging is shown as a function of tumor contrast, tumor size, and tumor local characteristics. Also, the performance of the proposed statistical decision based algorithm is compared to another one that post processes reconstructed images of breast permittivity[2]. These results demonstrate the advantages of incorporating the microwave diffraction measurements directly into the computer-aided algorithm design.

[1] In the simulation, the microwave diffraction measurements are computed using the Extended Born Approximation (EBA) accelerated CGFFT method (proposed by Zhang and Liu) with an ensemble of simulated breast permittivity images as the propagating media.

[2] The reconstructed permittivity images are obtained using back-propagation following by Contrast Source Inversion (CSI, Berg), which was proposed by Zhang and Liu.

2 QUANTITATIVE PERFORMANCE EVALUATION

Receiver Operating Characteristic (ROC)

- Probability of Correct Detection (P_D) as a function of Probability of False Alarm (P_F) $P_F = \int_\beta d\lambda p(\lambda | H_0)$ $P_D = \int_\beta d\lambda p(\lambda | H_1)$
- ROC's are obtained in general through simulations of λ under H_1 and H_0 conditions.

Detectability (or Deflection Coefficient) d

- d characterizes the ROC curve for the detection problem of signal known exactly plus white Gaussian noise, where P_D = 1-Gau2cdf(Gau2inv(1-P_F)-d).
- Here, d is estimated from the ROC curve. Each point on the Detectability curve represents an approximation to one ROC curve.

Probability of Correct Localization (PCL)

- PCL is the ratio of correct localization counts over total trials
- A correct localization means that the tumor is localized inside the target window
- The target window is a circle with fixed radius (pixels).

1 APPROACH

Post-Reconstruction Algorithm

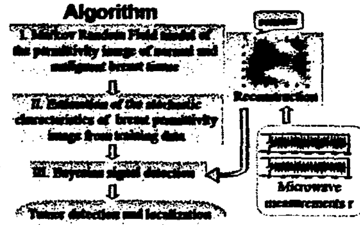

Proposed Algorithm

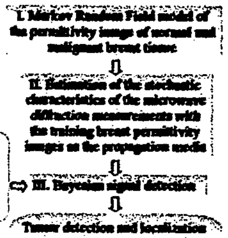

II Use the training set of breast permittivity images to estimate the model parameters, μ_1, μ_0, β_1 and β_0, and then transform to U,Q,U_s and Q_s, where $S \in \Omega$ (Ω is all possible tumor locations)

III Bayesian Processor for Uncertain Permittivity Image

Binary Hypotheses

$H_1: \varepsilon_r = T^{-1}(r | H_1)$, $r|H_1 = T(\varepsilon_o|H_1) + n$, $n \in C^K$, $n \sim N(0, 2\sigma_n^2 I_K)$

$H_0: \varepsilon_r = T^{-1}(r | H_0)$, $r|H_0 = T(\varepsilon_o|H_0) + n$, $T^{-1}: C^K \to R^{M \times M}$

ε_o original breast permittivity image, r measurements, ε_r reconstructed image

BP_UPI Detector

$$\lambda(\varepsilon_r) = \sum_{S\in\Omega} |Q_S| \exp\left(\frac{(\varepsilon_r - U)^T Q(\varepsilon_r - U) - (\varepsilon_r - U_S)^T Q_S(\varepsilon_r - U_S)}{2}\right)$$

BP_UPI Localization processor

$$\hat{S} = \max_{S\in\Omega} p(S|\varepsilon_r) = \max_{S\in\Omega} |Q_S| \exp\left(-\frac{(\varepsilon_r - U_S)^T Q_S(\varepsilon_r - U_S)}{2}\right)$$

Bayesian Signal Detection Basics

Optimum detector for binary hypotheses
- The likelihood ratio of the data vector X followed by a threshold which is determined by the optimum criterion.

$$\Lambda(X) = \frac{p(X | H_1)}{p(X | H_0)}$$

Optimum localization processor
- The maximum a posteriori probability density function of the malignant tumor location given the data vector X.

$$\hat{S} = \max_{S\in\Omega} p_{S|X}(S|X)$$

I Local characteristic of breast permittivity

Gaussian Markov Random Field (GMRF Chellappa, 1985)

$$p(\varepsilon_{rij} | \varepsilon_{rkl} \in N_{ij}) = \frac{\exp\left(-\frac{1}{2\sigma_{ij}^2}(\varepsilon_{rij} - (\mu_{ij} - \sum_{kl\in N_{ij}} \beta_{ij,kl}(\varepsilon_{rkl} - \mu_{kl})))^2\right)}{\sqrt{2\pi\sigma_{ij}^2}}$$

(i,j), pixel in image; N_{ij}, neighborhood of (i,j); μ_{ij}, mean permittivity at pixel (i,j); $\beta_{ij,kl}$, interaction coefficient (kl)→(i,j)

The β matrix defines a 2M+1 x 2M+1 neighborhood system

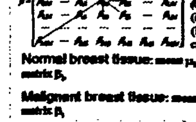

Normal breast tissue: mean μ_0, interaction coefficient matrix β_0

Malignant breast tissue: mean μ_1, interaction coefficient matrix β_1

Global characteristic of breast permittivity

$$p(\varepsilon_r) = \frac{|Q|^{1/2}}{2\pi^{N^2/2}} \exp\left(-\frac{(\varepsilon_r - U)^T Q(\varepsilon_r - U)}{2}\right)$$

No tumor present
Q: $N^2 \times N^2$, composed of β_0 or 0
U: $N^2 \times 1$, composed of μ_0

Tumor present at location S
Q_S: $N^2 \times N^2$, composed of β_0, β_1 or 0
U_S = (μ_1-μ_0) x tumor mean function + μ_0

An example of tumor mean function

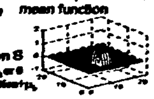

Some realizations of breast permittivity image

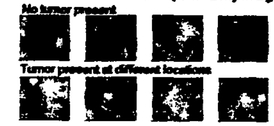

II Use the training set of breast permittivity images as the realizations of the propagating media to compute the forward propagation fields $T(\varepsilon_r)$ at known sensors.

Then estimate the mean vector and covariance matrix of $T(\varepsilon_r)$: (M,C) and (M_S,C_S) for H_0 and H_1 conditions respectively.

III Bayesian Processor for Scattered EM Field of Uncertain Permittivity Image

Binary Hypotheses: H_1: $r = T(\varepsilon_o | H_1) + n$, $r, n \in C^K$, $n \sim N(0, 2\sigma_n^2 I_K)$
H_0: $r = T(\varepsilon_o | H_0) + n$, $T: R^{M \times M} \to C^K$

BP_SEUPI detector

$$\lambda(r) = \frac{\sum_{S\in\Omega} \int p(r | T(\varepsilon_o), H_1) p(T(\varepsilon_o) | H_1, S) d\varepsilon_o}{\int p(r | T(\varepsilon_o), H_0) p(T(\varepsilon_o) | H_0) d\varepsilon_o}$$

BP_SEUPI localization processor

$$\hat{S} = \max_{S\in\Omega} p(S|r) = \max_{S\in\Omega} \int p(r | T(\varepsilon_o), H_1) p(T(\varepsilon_o) | H_1, S) d\varepsilon_o$$

- High dimensional integral is simplified by using multivariate complex Gaussian distribution as an approximation to p(T(ε_o)|H_i, i=0,1), which is called LBP_SEUPI (Low order BP_SEUPI)

LBP_SEUPI detector

$$\lambda(r) = \sum_{S\in\Omega} |C_1||C_{S1}|^{-1} \exp(M_{S1}^H C_{S1} M_{S1} - M_S^H C_S M_S - M_1^H C_1 M_1)$$

- $M_1 = C_1^{-1}(r/2\sigma_n^2 + CM)$, $C_1 = I/2\sigma_n^2 + C$

LBP_SEUPI localization processor

$$\hat{S} = \max_{S\in\Omega} |C_S||C_{S1}|^{-1} \exp(M_{S1}^H C_{S1} M_{S1} - M_S^H C_S M_S)$$

- $M_{S1} = C_{S1}^{-1}(r/2\sigma_n^2 + C_S M_S)$, $C_{S1} = I/2\sigma_n^2 + C_S$

2.1 PERPORMANCE UPPER BOUND

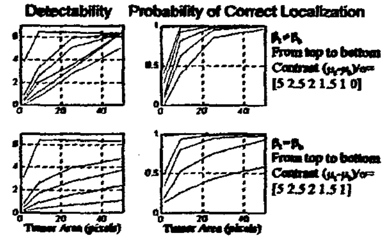

◆ Performance upper bound is obtained by training BP_PUI with the set of original breast permittivity images, and then testing it using another data set generated from the same model.

◆ Both the detection and localization performances increase with the tumor contrast and the tumor size; capturing different local patterns of breast tumor and normal background improves the diagnosis performance.

Simulation Configurations
- Image Size: 9.2x9.2cm², 529 pixels
- Tumor Size: various from 0.4x0.4cm² to 2.8x2.8cm² i.e.1 pixel to 49 pixels
- Tumor locations: uniformly distributed
- μ_0=30, μ_1 various in [30,35]
- β_1≠β_0 or β_1=β_0

$$\beta_0 = \begin{bmatrix} 1 & -0.1879 & 0.0191 \\ -0.1879 & -0.1724 & 0.0453 \\ 0.0191 & 0.0453 & 0.0007 \end{bmatrix} \quad \beta_1 = \begin{bmatrix} 1 & 0.1 \\ 0.1 & 0.1 \end{bmatrix}$$

Assuming symmetric property, only the lower right corner of the β matrix is shown

2.2 PERPORMANCE COMPARISON

Breast Tumor Detection Performance

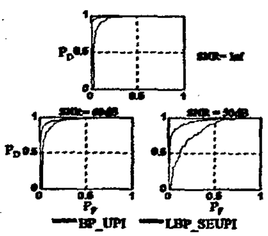

◆ Both algorithms have good detection performance when SNR ≥60dB

◆ LBP_SEUPI (proposed algorithm) is better than BP_UPI (post-reconstruction algorithm) for all three SNR's

Breast Tumor localization Performance

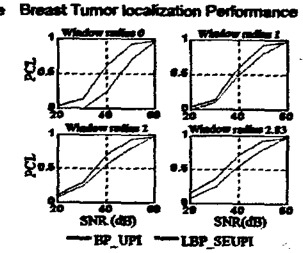

◆ Localization performance increases as a function of SNR

◆ PCL close to 1 at 60dB SNR for both algorithms

◆ LBP_SEUPI is better than BP_UPI for all four window configurations

An example of breast tumor localization

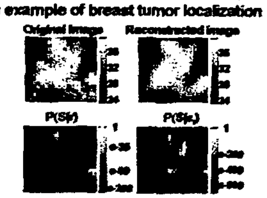

◆ It is not easy to locate the tumor in the reconstructed image by eye

◆ P(S|r) (Proposed algorithm) got the right tumor location.

◆ P(S| ε_r=T^{-1}(r)) made a mistake.

Simulation Configurations
- Image Size: 9.2x9.2cm², 529 pixels
- Tumor Size: 2x2cm², 25 pixels
- Tumor locations: uniformly distributed
- μ_0=30, μ_1= 40, β_1≠β_0
- SNR = $T(\varepsilon_o)^H T(\varepsilon_o) / \sigma_n^2$

SUMMARY

- Decision-aided breast tumor diagnostic algorithms based on signal detection theory and microwave energy, which has no radiation danger at low power levels, have the potential of providing additional information for radiologist so as to improve the probability of detection of breast tumors as well as their correct locations.
- The LBP_SEUPI gains better performance than the BP_UPI by modeling the microwave measurements as a function of the random propagating medium, and making decisions before the reconstruction procedure.
- Tumor detection and localization performance upper bounds, in terms of the ROC and PCL, are given as a function of tumor characteristics, including the malignant/normal permittivity contrast and tumor area.

This research was supported by the U.S. Army Medical Research Center under DAMD17-01-1-0513

[This page is intentionally left blank.]